JCTC Journal of Chemical Theory and Computation

pubs.acs.org/JCTC Article

Steering Active-Colloid Assembly by Biasing Dissipation

Chaoqun Du, Zhiyu Cao,* and Zhonghuai Hou*

Cite This: https://doi.org/10.1021/acs.jctc.6c00384 Read Online

ACCESS | Metrics & More | Article Recommendations | Supporting Information

ABSTRACT: Complex nonequilibrium self-assembly enables the formation of materials with specific patterns and functions from the bottom up. How to directionally control the assembly to form the target configuration is a challenge. Here, we propose a dissipation bias principle for targeted assembly, which highlights that controlling the dissipation tendency can play an important role in modulating the frequency and intensity of local rearrangements. Following this principle, one can induce ordered target configurations from disordered structures and achieve directional selection among multiple assembly pathways. We used the assembly of active colloids as a platform to show our results.

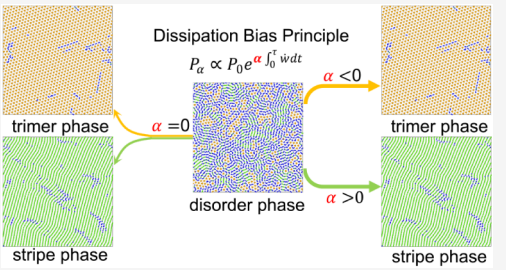

INTRODUCTION

Self-assembly refers to the autonomous organization of components into patterns or structures, which is an ideal approach to achieving complex organization and an important research subject in biochemistry.[1] In complex self-assemblies, precise control over interactions among components is required to achieve the desired structures. Such control includes tuning the concentration of components, as well as the specificity and strength of interactions, among other factors. Additionally, due to the dynamic nature of the system, interactions between components may lead to heterogeneity or competitive phenomena, thereby influencing the final structure and performance. In equilibrium states, even though target structures are encoded through specific interactions,[2−7] the system can still easily fall into kinetic trapping states with numerous defects, especially in high-density self-assembly systems.[8,9] Therefore, dynamic control of targeted self-assembly processes remains a major challenge.

A common strategy widely used in nature is to bypass the entropy bottleneck through energy input, which can assemble features that are impossible to appear in equilibrium states, and it can even be multitarget states.[10] However, without control over the dissipative trends, the system still tends to form random components that are not adapted to the environment.[11−14] Here, we employed a biased ensemble approach to demonstrate that controlling the dissipation tendency quantitatively constitutes a dissipation bias principle for complex self-assembly. The biased ensemble approach is built based on stochastic thermodynamics[15−23] and large deviation theory[16,18,19,21−27] regularly monitoring the dissipation during the assembly process of replicas. This approach can effectively capture energy-avoiding/seeking paths and gradually collect the energy-avoiding/seeking states, ultimately linking to the targeted configuration. At the statistical level, controlling the dissipation tendency regulates the frequency and intensity of local structural rearrangements, which lead to renormalized interactions. Following the principle we proposed, one can not only induce the emergence of targeted ordered configurations from disordered structures but also directionally select targeted configurations from multiple assembly pathways. We demonstrated our dissipation bias principle using the assembly of active colloids as a platform.

MODEL

First, we reproduced the stripe phase and trimer phase observed in experiments[28−30] through the molecular dynamics simulation of N active core−corona particles (ACCPs) in two dimensions (2D). The so-called core−corona colloids are a type of particle with a nanoparticle core and polymer or gel coatings on the surface,[31] which are capable of producing rich structures with unusual symmetry.[30,32−35] Figure 1a shows a schematic diagram of the ACCP particle. The core with a diameter of σ simulates the impenetrable hard core of the ACCP. Its interactions are

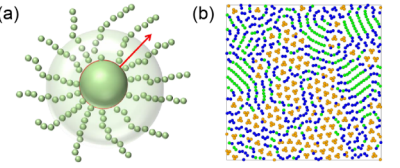

Figure 1. (a) Sketch of the model of the active core−corona particles (ACCPs). (b) The typical configuration of the ACCP assembly system with the disordered phase (blue), stripe phase (green), and trimer phase (orange) in the steady states.

Received: March 2, 2026
Revised: April 15, 2026
Accepted: April 16, 2026

described by the Weeks−Chandler−Andersen (WCA) interaction potential: $U_{core}(r_{ij}) = 4\varepsilon[(\sigma/r_{ij})^{12} - (\sigma/r_{ij})^6 + 1/4]$ for $r_{ij} < 2^{1/6}\sigma$, and $U_{core}(r_{ij}) = 0$ otherwise, where ε is the interaction strength. As for the outer shell, we use Hookean springs to simulate its interactions,[36] given by $U_{corona}(r_{ij}) = k_s(r_{ij} - r_c)^2/2$ for $r_{ij} < r_c$, and $U_{corona}(r_{ij}) = 0$ otherwise, similar to the soft repulsion between soft-core particles formed by microgels.[8] k_s is the strength of the spring potential, and r_c is the cutoff distance. Each colloid undergoes Brownian dynamics at a constant temperature T, described by the coupled overdamped equations:

$$\dot{\boldsymbol{r}}_i = \mu \boldsymbol{F}_i + v_0 \boldsymbol{u}(\theta_i) + \sqrt{2D_t}\boldsymbol{\eta}_i; \qquad \dot{\theta}_i = \sqrt{2D_r}\,\xi_i \tag{1}$$

where μ represents the particle's mobility, and $\boldsymbol{\eta}_i$, ξ_i are zero-mean, unit-variance Gaussian white noises. D_t and D_r are the translational and rotational diffusivities, respectively. The active driving term is introduced through a self-propulsion speed of constant magnitude v_0 and is modeled along a predefined orientation vector $\boldsymbol{u}(\theta_i) = (\cos\theta_i, \sin\theta_i)$, which passes through the particle's center of mass.

The system in the simulation exhibits different structures for different values of the spring potential strengths (k_s) and the self-propulsion speed (v_0). Figure 1b shows three characteristic configurations that exist in the parameter space: the disordered phase (blue), the stripe phase (green), and the trimer phase (orange). To identify which phase a particle belongs to, we evaluate the angle θ ($0° < \theta < 180°$) formed by the particle and its two nearest neighbors. A particle is classified as belonging to the stripe phase if $\theta > 160°$, to the trimer phase if $50° < \theta < 70°$, and to the disordered phase otherwise.

Dissipation Bias Principle

For active colloids, dissipation can be characterized by the average power input of the self-propelled force:[17−20]

$$\dot{\omega} = \frac{1}{N\tau}\sum_{i}^{N}\int_0^\tau \dot{w}_i \mathrm{d}t = \frac{v_0}{N\mu\tau}\sum_{i=1}^{N}\int_0^\tau \dot{\boldsymbol{r}}_i \circ \boldsymbol{u}(\theta_i)\,\mathrm{d}t \tag{2}$$

which naturally measures how efficiently active components create motion through energy consumption. Here, τ is the time duration, and $\circ$ represents the Stratonovich convention.

Here, we find that the target state is sensitive to the power input; systems are usually disordered when the dissipation tendency is not controlled. On the one hand, when the active power input is too small, the repulsion of the surface layer strongly inhibits the adjustment of the local structure. The motion of clusters formed by a small number of particles with low energy barriers, which act as quasi-particles, leads to spatially heterogeneous dynamics, and the system quickly relaxes to a steady state with a large number of defects.[37] Thus, the disordered structure dominates in this regime. On the other hand, when the active power input is too large, the system is more inclined to form isotropic disordered structures rather than the targeted ordered state because of the excessively intense local rearrangements. Therefore, there is an optimal dissipation for the assembly state to remain stable. At the statistical level, the optimal dissipation for maximizing the yield of targeted states arises from a moderate level of local rearrangements, which requires controlling the system's dissipation tendency (see Figure S2).

The large deviation theory and biased sampling approaches[38−42] offer us a framework to achieve control over the dissipative tendency in the simulation. By choosing the trajectory-dependent active power input as the observable, we employ the cloning algorithm to generate biased trajectories,[43,44] as schematically illustrated in Figure 2. The probability of biased trajectories is given by

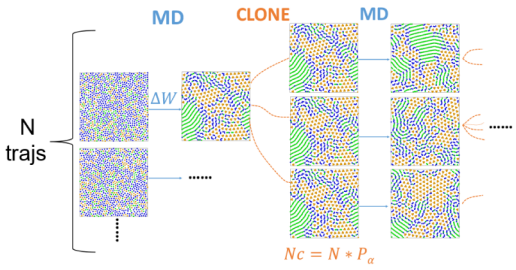

Figure 2. Schematic of the cloning algorithm for dissipation-biased trajectory sampling. A population of N trajectories is propagated in parallel by unbiased MD for a time window τ. At the end of each window, each trajectory is assigned a statistical weight P_α determined by the dissipation ΔW accumulated over τ. The population is then resampled by cloning or pruning trajectories in proportion to P_α and the number of clones is N_c.

$$P_\alpha \propto P_0 e^{\alpha\dot{\omega}\tau} \tag{3}$$

Here, P_0 is the probability of unbiased trajectories. We use the parameter α to bias sample trajectories according to active power input, thereby controlling the system's dissipation tendency. Positive values of α sample energy-seeking paths with high dissipation during the assembly process, while negative values sample energy-avoiding paths with low dissipation during the assembly process. By monitoring the system's response to the control of dissipation tendency at fixed periods, we can obtain trajectories corresponding to pumping active power into colloidal units or extracting energy from them at a specific rate. At the statistical level, controlling the dissipation tendency modulates the intensity and frequency of the local structure rearrangement, which effectively renormalizes the interaction. In practice, we propagate a population of $N_{traj} = 100$ trajectories in parallel over a time window $\tau = 5 \times 10^3$. At the end of each window, the active power accumulated along each trajectory is used to assign its statistical weight, and the population is then resampled by cloning or pruning accordingly. More details are provided in the Supporting Information.

INDUCE ORDERED TARGET CONFIGURATIONS FROM THE DISORDERED PHASE

In the following, we show how the dissipation bias principle guides complex self-assembly processes in two representative scenarios. In the first scenario, we show that controlling the dissipation tendency can generate ordered trimer structures from disordered phases while improving their stability. We focus on the parameters with $v_0 = 70$ and $k_s = 190$, a regime in which the uncontrolled dynamics ($\alpha = 0$) remain largely disordered. At $\alpha = 0$, the trimer yield remains low at ~0.1, although trimer-rich local rearrangement clusters intermittently emerge, with yields reaching up to ~0.4. Interestingly, the dissipation drops precisely when trimer order emerges, indicating that the dissipation tendency provides a direct control handle (Figure 3a). Following our proposed dissipation bias principle, we set a negative α ($\alpha = -1$) to suppress the system's dissipation tendency and stabilize the emergent trimer structures. By

https://doi.org/10.1021/acs.jctc.6c00384
J. Chem. Theory Comput. XXXX, XXX, XXX−XXX

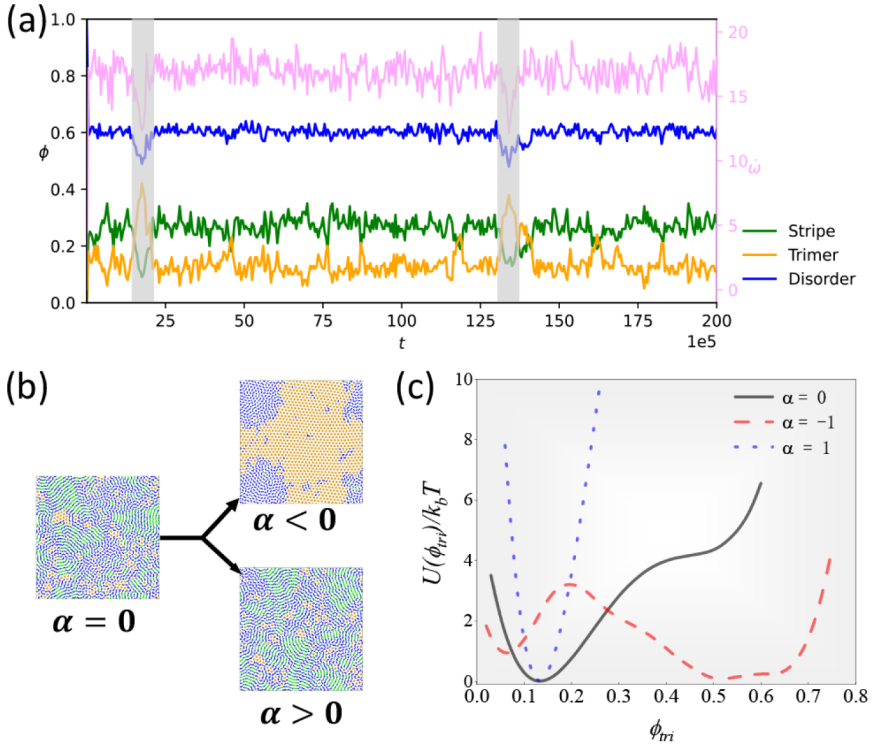

Figure 3. (a) The temporal emergence of an ordered trimer cluster from a disordered structure is accompanied by a sudden drop in dissipation, highlighted by the gray-shaded region. We show the time series of the yields of the three states together with the active power input. (b) Representative simulation snapshots for different α. Middle-left: no control of the dissipation tendency ($\alpha = 0$). Upper-right: energy-avoiding pathways ($\alpha = -1$). Lower-right: energy-seeking pathways ($\alpha = 1$). Parameters: $v_0 = 70$ and $k_s = 190$. (c) The effective energy profiles along the reaction coordinate ϕ_{tri}. Black solid line: no control. Red dashed line: $\alpha = -1$. Blue dotted line: $\alpha = 1$.

repeatedly iterating the procedure shown in Figure 2, the ensemble becomes progressively enriched through energy-avoiding pathways, which in turn steer the system toward an ordered configuration. In this regime, suppressing dissipation tendencies gives rise to additional energy punishment, which leads to emergent spinodal stability. Therefore, trimer-rich clusters with lower dissipation can persist, leading to a marked increase in trimer yield, which can reach ∼0.7 for $\alpha < 0$ (see Figure 3b and Figure S5). In contrast, a positive bias ($\alpha > 0$) increases the dissipation tendency and promotes more dissipative dynamics, thereby suppressing the assembly of the trimer configurations (see Figure S5).

To further clarify our findings, we construct an effective energy landscape $U(\phi_{tri}) = -k_BT \ln P_{ss}(\phi_{tri})$ from steady-state trajectory data by estimating $P_{ss}(\phi_{tri})$ (see the SI for details). As shown in Figure 3c, this representation makes the impact of dissipation-tendency control explicit. At $\alpha = 0$, $U(\phi_{tri})$ displays a single stable minimum near $\phi_{tri} \simeq 0.1-0.2$. When the dissipation tendency is suppressed ($\alpha = -1 < 0$), an additional basin can be observed on the high-ϕ_{tri} side ($\phi_{tri} \simeq 0.6$), indicating the stabilization of trimer-rich structures. In contrast, enhancing the dissipation tendency ($\alpha = 1 > 0$) deepens and steepens the low-ϕ_{tri} basin, thereby suppressing the emergence of trimer-rich clusters.

To further clarify our findings, we construct an effective energy landscape (or effective potential of mean force) along the reaction coordinate ϕ_{tri},

$$U(\phi_{tri}) = -k_BT \ln P_{ss}(\phi_{tri})$$

from the steady-state distribution $P_{ss}(\phi_{tri})$ estimated from trajectory data (see SI for details). We need to emphasize that this effective landscape is useful for visualizing basin preference but not sufficient on its own to fully characterize the kinetics, because nonequilibrium probability currents may persist, and the full dynamics cannot generally be reduced to gradient descent on this landscape alone. As shown in Figure 3c, this representation makes the impact of dissipation-tendency control explicit. At $\alpha = 0$, $U(\phi_{tri})$ displays a single stable minimum near $\phi_{tri} \simeq 0.1-0.2$. When the dissipation tendency is suppressed ($\alpha = -1 < 0$), an additional basin can be observed at the high-ϕ_{tri} side ($\phi_{tri} \simeq 0.6$), consistent with the stabilization of trimer-rich structures. In contrast, enhancing the dissipation tendency ($\alpha = 1 > 0$) deepens and steepens the low-ϕ_{tri} basin, thereby reducing the statistical weight of trimer-rich clusters. We emphasize that in the absence of bias, the system is not in a regime where trimer states are stably sustained. Instead, the dynamics are dominated by strong active rearrangements that continuously disrupt locally ordered structures. The introduction of a dissipation bias dynamically stabilizes trimer configurations that would otherwise remain transient, thereby giving rise to a regime in which trimer-rich and trimer-disordered regions coexist in our simulations.

DIRECTIONALLY SELECTING AMONG MULTIPLE ASSEMBLY PATHWAYS

In the second scenario, we demonstrate that controlling dissipation tendencies provides an effective route to directed assembly. Multiple assembly pathways can coexist under the same conditions, resulting in distinct long-lived ordered outcomes, as observed in nature, experiments, and simulations.[45,46] How to achieve directed assembly in multiple pathways is a challenge. Systems with competing dynamical

https://doi.org/10.1021/acs.jctc.6c00384
J. Chem. Theory Comput. XXXX, XXX, XXX−XXX

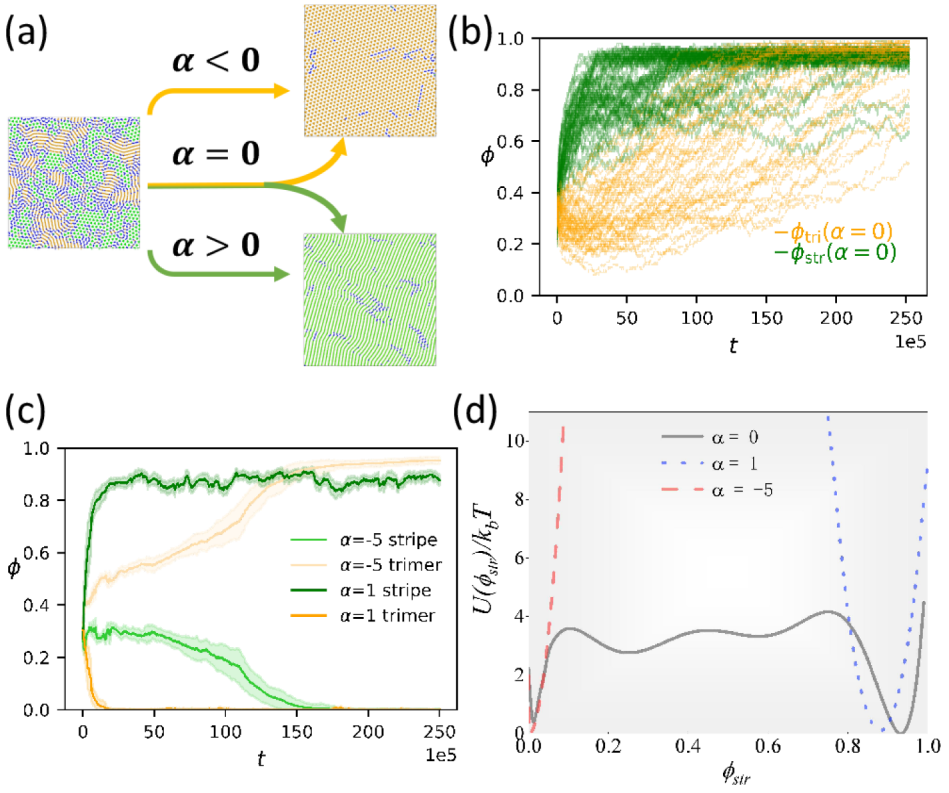

Figure 4. (a) Representative snapshots from simulations for different α. When there is no control of the dissipation tendency with $\alpha = 0$, the system will assemble into both stripe-ordered and trimer-ordered configurations through two different assembly pathways. On the one hand, for $\alpha = -5 < 0$, the energy-avoiding pathways will be collected. Particles directionally assemble into the trimer state with low dissipation. On the other hand, for $\alpha = 1 > 0$, the energy-seeking path will be collected. Particles assemble into the stripe structure with high dissipation. (b) Time series of ϕ_{str} (green) and ϕ_{tri} (orange) measured along 100 independent trajectories with $\alpha = 0$. Each curve corresponds to one trajectory. The parameters are: $v_0 = 40$ and $k_s = 220$. (c) Time series of the trimer yield (orange) and the stripe yield (green). The curves are averaged over the trajectory population, and the shaded bands represent the fluctuations calculated from multiple realizations (each realization has 100 trajectories in the cloning algorithm). Values of α: $\alpha = 1$ (light) and $\alpha = -5$ (dark). The parameters are: $v_0 = 40$ and $k_s = 220$. (d) The effective energy profiles of the system over the reaction coordinate ϕ_{str}. Black solid line: no control. Red dashed line: $\alpha = -5$. Blue dotted line: $\alpha = 1$.

pathways are sensitive to fluctuations, meaning that even identical initial conditions can lead to different ordered structures—a phenomenon indicative of replica symmetry breaking.[47] At $v_0 = 40$ and $k_s = 220$, simulations of $N_{traj} = 100$ trajectories starting from random initial configurations resulted in either trimer or stripe configurations, which occurred with nearly equal likelihood (51 stripes versus 49 trimers; see Figure 4b). Both configurations serve as stable attractors for the system, and transitions between stable states are not observed within the simulation's time scale. Interestingly, we quantify dissipation by calculating the active power input and find a distinct hierarchy: the dissipation associated with the stripe configuration is greater than that of the trimer configuration (see the Supporting Information). The significant difference in dissipative behavior between the stripe and trimer conformations provides us with a direct control handle. Following our proposed dissipation bias principle, we achieved directional self-assembly of the stripe and trimer configurations (Figure 4a). We set $\alpha < 0$ to suppress the system's dissipation tendency, thereby steering it along an energy-avoiding pathway that inhibits the formation of the highly dissipative stripe conformation and ultimately promotes the low-dissipation trimer configuration. Interestingly, there exists an optimal dissipation-bias strength for maximizing the yield of the targeted structure (see the Supporting Information). This is because the magnitude of α controls the intensity of local rearrangements: moderate bias facilitates ordered assembly, whereas excessively strong bias leads to excessively frequent or overly disruptive rearrangements that reduce the regularity of the emerging pattern. This is akin to the phenomenon reported by Rana and Barato in the context of Turing patterns, where an optimal level of dissipation is required to achieve the most regular spatial patterns.[48] Such an optimal level of dissipation for achieving optimal function has also been observed in other nonequilibrium living systems.[49,50] In contrast, when $\alpha > 0$ is applied to enhance dissipation, the system follows an energy-seeking pathway and eventually converges to the stripe configuration. Once dissipation tendency control is introduced, the originally bistable assembly routes collapse into a single directional pathway that can reliably connect to the targeted configuration. The time series of the yields of the trimer and stripe structures are shown in Figure 4c.

To further clarify our findings, we reconstruct the effective energy landscape $U(\phi_{str})$. At $\alpha = 0$, $U(\phi_{str})$ exhibits a bistable profile with two well-separated basins: a low-ϕ_{str} basin around $\phi_{str} \approx 0.05$ and a high-ϕ_{str} basin around $\phi_{str} \approx 0.9$, consistent with two long-lived attractors and hence competing assembly pathways. Suppressing the dissipation tendency ($\alpha = -5 < 0$) strongly favors the low-ϕ_{str} basin while destabilizing the high-ϕ_{str} basin, whereas enhancing it ($\alpha = 1 > 0$) instead stabilizes the high-ϕ_{str} basin and penalizes low ϕ_{str}. In both cases, the control effectively tilts the landscape to remove pathway competition, yielding a predominantly single-funnel route toward the target

https://doi.org/10.1021/acs.jctc.6c00384
J. Chem. Theory Comput. XXXX, XXX, XXX−XXX

configuration. The above results are robust against the population and frequency of the cloning algorithm, N_{traj} and τ, respectively (see Supporting Information for more details).

SUMMARY AND DISCUSSION

We construct a dissipation-biased ensemble of nonequilibrium assembly trajectories within a large-deviation framework and realize it numerically by using a cloning algorithm that periodically reweights trajectories according to their active power. The resulting biased ensemble should be understood as a statistical-mechanical construction that identifies trajectory classes with different dissipation tendencies. In this sense, our approach is closely related to earlier studies of trajectory-biased and activity-biased ensembles in active and nonequilibrium systems.[22,51] The conceptual distinction here is that the biased ensemble is used not primarily as a diagnostic tool for rare fluctuations but as a framework for formulating a control principle for targeted nonequilibrium self-assembly. Within this framework, the dissipation tendency becomes an explicit control parameter. It acts directly on the kinetic bottleneck associated with local rearrangements by modulating both their occurrence rate and their typical strength, thereby reshaping the effective landscape in a way that cannot be achieved by static interaction design alone. Our framework is also complementary to variational or optimization-based approaches for nonequilibrium design.[24,52] Rather than directly optimizing microscopic interactions or prescribing a control field from the outset, we identify the dissipation tendency as a physically meaningful coarse-grained variable that organizes the assembly dynamics and indicates which classes of trajectories favor a desired structure.

With the rapid development of control technologies that increasingly enable external energy injection to be programmed in space and time, regulating the dissipation tendency is becoming experimentally feasible. In this context, the dissipation-biased ensemble should be viewed as a principle for control rather than a literal laboratory protocol. By tuning the rate and spatiotemporal pattern of energy injection, one can bias the system toward trajectory classes with different dissipation tendencies and, thereby, favor different assembly basins. Although energy injection does not necessarily increase a system's dissipation tendency, it nevertheless provides a practical handle for tuning it. For example, dissipation tendency can be tuned by modulating ATP concentration in biological systems[53−57] or by controlling pH in chemical systems to regulate chemical energy input;[58] it can also be regulated through designed reactions and recombination/mutation-like processes in building blocks.[54,59] Active colloids provide a particularly direct platform for controllable self-assembly, in which local energy injection can be engineered to tune dissipation tendency[60−72] while nonequilibrium DNA systems offer a complementary route, in which adaptive and programmable structures can be achieved by synchronizing energy-seeking or energy-avoiding events with bond formation or cleavage.[73]

ASSOCIATED CONTENT

Supporting Information

The Supporting Information is available free of charge at https://pubs.acs.org/doi/10.1021/acs.jctc.6c00384.

Detailed simulation methods, parameter settings, and additional simulation snapshots (PDF)

AUTHOR INFORMATION

Corresponding Authors

Zhiyu Cao − *Center for Theoretical Biological Physics, Rice University, Houston, Texas 77005, United States*; Email: zc61@rice.edu

Zhonghuai Hou − *Department of Chemical Physics, University of Science and Technology of China, Hefei, Anhui 230026, China; Hefei National Research Center for Physical Sciences at the Microscale, Hefei, Anhui 230026, China*; orcid.org/0000-0003-1241-7041; Email: hzhlj@ustc.edu.cn

Author

Chaoqun Du − *Department of Chemical Physics, University of Science and Technology of China, Hefei, Anhui 230026, China*; orcid.org/0009-0001-4728-0383

Complete contact information is available at: https://pubs.acs.org/10.1021/acs.jctc.6c00384

Notes

The authors declare no competing financial interest.

ACKNOWLEDGMENTS

C. D. and Z. H. were supported by MOST-NSFC (2022YFA1303100 and 22533005) and the Fundamental and Interdisciplinary Disciplines Breakthrough Plan of the Ministry of Education of China (JYB2025XDXM505).

REFERENCES

(1) Whitesides, G. M.; Grzybowski, B. Self-assembly at all scales. *Science* **2002**, *295*, 2418−2421.

(2) Erb, R. M.; Son, H. S.; Samanta, B.; Rotello, V. M.; Yellen, B. B. Magnetic assembly of colloidal superstructures with multipole symmetry. *Nature* **2009**, *457*, 999−1002.

(3) Sacanna, S.; Irvine, W. T.; Chaikin, P. M.; Pine, D. J. Lock and key colloids. *Nature* **2010**, *464*, 575−578.

(4) Chen, Q.; Bae, S. C.; Granick, S. Directed selfassembly of a colloidal kagome lattice. *Nature* **2011**, *469*, 381−384.

(5) Wang, Y.; Wang, Y.; Breed, D. R.; Manoharan, V. N.; Feng, L.; Hollingsworth, A. D.; Weck, M.; Pine, D. J. Colloids with valence and specific directional bonding. *Nature* **2012**, *491*, 51−55.

(6) Damasceno, P. F.; Engel, M.; Glotzer, S. C. Predictive self-assembly of polyhedra into complex structures. *Science* **2012**, *337*, 453−457.

(7) Manoharan, V. N. Colloidal matter: Packing, geometry, and entropy. *Science* **2015**, *349* (6251), 1253751.

(8) Rey, M.; Law, A. D.; Buzza, D. M. A.; Vogel, N. Anisotropic self-assembly from isotropic colloidal building blocks. *J. Am. Chem. Soc.* **2017**, *139*, 17464−17473.

(9) Bodnarchuk, M. I.; Shevchenko, E. V.; Talapin, D. V. Structural defects in periodic and quasicrystalline binary nanocrystal superlattices. *J. Am. Chem. Soc.* **2011**, *133*, 20837−20849.

(10) Bisker, G.; England, J. L. Nonequilibrium associative retrieval of multiple stored self-assembly targets. *Proc. Natl. Acad. Sci. U. S. A.* **2018**, *115* (45), No. E10531-E10538.

(11) Boekhoven, J.; Hendriksen, W. E.; Koper, G. J.; Eelkema, R.; van Esch, J. H. Transient assembly of active materials fueled by a chemical reaction. *Science* **2015**, *349*, 1075−1079.

(12) Carnall, J. M.; Waudby, C. A.; Belenguer, A. M.; Stuart, M. C.; Peyralans, J. J.-P.; Otto, S. Mechanosensitive self-replication driven by self-organization. *Science* **2010**, *327*, 1502−1506.

(13) Sadownik, J. W.; Mattia, E.; Nowak, P.; Otto, S. Diversification of self-replicating molecules. *Nat. Chem.* **2016**, *8*, 264−269.

(14) Tena-Solsona, M.; Rieß, B.; Grötsch, R. K.; Löhrer, F. C.; Wanzke, C.; Käsdorf, B.; Bausch, A. R.; Müller-Buschbaum, P.; Lieleg,

O.; Boekhoven, J. Nonequilibrium dissipative supramolecular materials with a tunable lifetime. *Nat. Commun.* **2017**, *8* (1), 15895.
(15) Seifert, U. Stochastic thermodynamics, fluctuation theorems and molecular machines. *Rep. Prog. Phys.* **2012**, *75*, 126001.
(16) Tociu, L.; Fodor, É.; Nemoto, T.; Vaikuntanathan, S. How dissipation constrains fluctuations in nonequilibrium liquids: Diffusion, structure, and biased interactions. *Phys. Rev.* **2019**, *9*, 041026.
(17) Pietzonka, P.; Fodor, É.; Lohrmann, C.; Cates, M. E.; Seifert, U. Autonomous engines driven by active matter: Energetics and design principles. *Phys. Rev.* **2019**, *9* (4), 041032.
(18) Cagnetta, F.; Corberi, F.; Gonnella, G.; Suma, A. Large fluctuations and dynamic phase transition in a system of self-propelled particles. *Phys. Rev. Lett.* **2017**, *119*, 158002.
(19) Nemoto, T.; Fodor, É.; Cates, M. E.; Jack, R. L.; Tailleur, J. Optimizing active work: Dynamical phase transitions, collective motion, and jamming. *Phys. Rev. E* **2019**, *99*, 022605.
(20) Cao, Z.; Su, J.; Jiang, H.; Hou, Z. Effective entropy production and thermodynamic uncertainty relation of active brownian particles. *Phys. Fluids* **2022**, *34* (5), 053310.
(21) Fodor, É.; Nemoto, T.; Vaikuntanathan, S. Dissipation controls transport and phase transitions in active fluids: mobility, diffusion and biased ensembles. *New J. Phys.* **2020**, *22*, 013052.
(22) Fodor, É.; Jack, R. L.; Cates, M. E. Irreversibility and biased ensembles in active matter: Insights from stochastic thermodynamics. *Ann. Rev. Condens. Matter Phys.* **2022**, *13*, 215−238.
(23) O'Byrne, J.; Kafri, Y.; Tailleur, J.; van Wijland, F. Time irreversibility in active matter, from micro to macro. *Nat. Rev. Phys.* **2022**, *4*, 167−183.
(24) Das, A.; Limmer, D. T. Variational design principles for nonequilibrium colloidal assembly. *J. Chem. Phys.* **2021**, *154* (1), 014107.
(25) Touchette, H. The large deviation approach to statistical mechanics. *Phys. Rep.* **2009**, *478*, 1−69.
(26) Jack, R. L. Ergodicity and large deviations in physical systems with stochastic dynamics. *Eur. Phys. J. B* **2020**, *93* (4), 74.
(27) Lamtyugina, A.; Qiu, Y.; Fodor, É.; Dinner, A. R.; Vaikuntanathan, S. Thermodynamic control of activity patterns in cytoskeletal networks. *Phys. Rev. Lett.* **2022**, *129*, 128002.
(28) Seul, M.; Andelman, D. Domain shapes and patterns: the phenomenology of modulated phases. *Science* **1995**, *267*, 476−483.
(29) Stoycheva, A. D.; Singer, S. J. Stripe melting in a two-dimensional system with competing interactions. *Phys. Rev. Lett.* **2000**, *84*, 4657.
(30) Malescio, G.; Pellicane, G. Stripe phases from isotropic repulsive interactions. *Nat. Mater.* **2003**, *2*, 97−100.
(31) Si, K. J.; Chen, Y.; Shi, Q.; Cheng, W. Nanoparticle superlattices: The roles of soft ligands. *Adv. Sci.* **2018**, *5* (1), 1700179.
(32) Dotera, T.; Oshiro, T.; Ziherl, P. Mosaic twolengthscale quasicrystals. *Nature* **2014**, *506*, 208−211.
(33) Portehault, D.; Cassaignon, S.; Nassif, N.; Baudrin, E.; Jolivet, J.-P. A core-corona hierarchical manganese oxide and its formation by an aqueous soft chemistry mechanism. *Angew. Chem., Int. Ed.* **2008**, *47*, 6441−6444.
(34) Jagla, E. Phase behavior of a system of particles with core collapse. *Phys. Rev. E* **1998**, *58*, 1478.
(35) Du, Y.; Jiang, H.; Hou, Z. Self-assembly of active core corona particles into highly ordered and self-healing structures. *J. Chem. Phys.* **2019**, *151* (15), 154904.
(36) Cheng, W.; Hartman, M. R.; Smilgies, D.-M.; Long, R.; Campolongo, M. J.; Li, R.; Sekar, K.; Hui, C.-Y.; Luo, D. Probing in real time the soft crystallization of dna-capped nanoparticles. *Angew. Chem., Int. Ed.* **2010**, *49*, 380−384.
(37) Nishikawa, Y.; Berthier, L. Collective relaxation dynamics in a three-dimensional lattice glass model. *Phys. Rev. Lett.* **2024**, *132*, 067101.
(38) Garrahan, J. P.; Jack, R. L.; Lecomte, V.; Pitard, E.; van Duijvendijk, K.; van Wijland, F. Dynamical firstorder phase transition in kinetically constrained models of glasses. *Phys. Rev. Lett.* **2007**, *98*, 195702.
(39) Hedges, L. O.; Jack, R. L.; Garrahan, J. P.; Chandler, D. Dynamic order-disorder in atomistic models of structural glass formers. *Science* **2009**, *323*, 1309−1313.
(40) Pitard, E.; Lecomte, V.; Van Wijland, F. Dynamic transition in an atomic glass former: A moleculardynamics evidence. *Europhys. Lett.* **2011**, *96*, 56002.
(41) Speck, T.; Engel, A.; Seifert, U. The large deviation function for entropy production: the optimal trajectory and the role of fluctuations. *J. Stat. Mech.: Theory Exp.* **2012**, *2012* (12), P12001.
(42) Chetrite, R.; Touchette, H. Nonequilibrium microcanonical and canonical ensembles and their equivalence. *Phys. Rev. Lett.* **2013**, *111*, 120601.
(43) Tailleur, J.; Kurchan, J. Probing rare physical trajectories with lyapunov weighted dynamics. *Nat. Phys.* **2007**, *3*, 203−207.
(44) Nemoto, T.; Bouchet, F.; Jack, R. L.; Lecomte, V. Population-dynamics method with a multicanonical feedback control. *Phys. Rev. E* **2016**, *93*, 062123.
(45) Ozbudak, E. M.; Thattai, M.; Lim, H. N.; Shraiman, B. I.; Van Oudenaarden, A. Multistability in the lactose utilization network of escherichia coli. *Nature* **2004**, *427*, 737−740.
(46) Li, Q.; Wennborg, A.; Aurell, E.; Dekel, E.; Zou, J.-Z.; Xu, Y.; Huang, S.; Ernberg, I. Dynamics inside the cancer cell attractor reveal cell heterogeneity, limits of stability, and escape. *Proc. Natl. Acad. Sci. U. S. A.* **2016**, *113*, 2672−2677.
(47) Mézard, M.; Parisi, G.; Virasoro, M. A. *Spin glass theory and beyond: An Introduction to the Replica Method and Its Applications*; World Scientific Publishing Company, 1987; Vol. *9*.
(48) Rana, S.; Barato, A. C. Precision and dissipation of a stochastic turing pattern. *Phys. Rev. E* **2020**, *102*, 032135.
(49) Cao, Z.; Bao, R.; Hou, Z. Cascade-enhanced transport efficiency of biochemical systems. *Chaos* **2023**, *33* (6), 063104.
(50) Cao, Z.; Jiang, H.; Hou, Z. Designing circle swimmers: Principles and strategies. *J. Chem. Phys.* **2021**, *155* (23), 234901.
(51) Das, A.; Kuznets-Speck, B.; Limmer, D. T. Direct evaluation of rare events in active matter from variational path sampling. *Phys. Rev. Lett.* **2022**, *128*, 028005.
(52) Das, A.; Limmer, D. T. Variational control forces for enhanced sampling of nonequilibrium molecular dynamics simulations. *J. Chem. Phys.* **2019**, *151* (24), 244123.
(53) England, J. L. Dissipative adaptation in driven selfassembly. *Nat. Nanotechnol.* **2015**, *10*, 919−923.
(54) Te Brinke, E.; Groen, J.; Herrmann, A.; Heus, H. A.; Rivas, G.; Spruijt, E.; Huck, W. T. Dissipative adaptation in driven self-assembly leading to self-dividing fibrils. *Nat. Nanotechnol.* **2018**, *13*, 849−855.
(55) Perunov, N.; Marsland, R. A.; England, J. L. Statistical physics of adaptation. *Phys. Rev. X* **2016**, *6* (2), 021036.
(56) Cao, Z.; Wolynes, P. G. Motorized chain models of the ideal chromosome. *Proc. Natl. Acad. Sci. U. S. A.* **2024**, *121* (28), No. e2407077121.
(57) Cao, Z.; Du, C.; Hou, Z.; Wolynes, P. G. Motorized chromosome models of mitotic chromosome folding. *Nat. Commun.* **2025**, *16* (1), 11085.
(58) Tagliazucchi, M.; Weiss, E. A.; Szleifer, I. Dissipative self-assembly of particles interacting through time-oscillatory potentials. *Proc. Natl. Acad. Sci. U. S. A.* **2014**, *111*, 9751−9756.
(59) Zwicker, D.; Seyboldt, R.; Weber, C. A.; Hyman, A. A.; Jülicher, F. Growth and division of active droplets provides a model for protocells. *Nat. Phys.* **2017**, *13*, 408−413.
(60) Aubret, A.; Youssef, M.; Sacanna, S.; Palacci, J. Targeted assembly and synchronization of self-spinning microgears. *Nat. Phys.* **2018**, *14*, 1114−1118.
(61) Mallory, S. A.; Cacciuto, A. Activity-enhanced selfassembly of a colloidal kagome lattice. *J. Am. Chem. Soc.* **2019**, *141*, 2500−2507.
(62) Mallory, S. A.; Valeriani, C.; Cacciuto, A. An active approach to colloidal self-assembly. *Annu. Rev. Phys. Chem.* **2018**, *69*, 59−79.
(63) Dey, K. K.; Wong, F.; Altemose, A.; Sen, A. Catalytic motors-quo vadimus? *Curr. Opin. Colloid Interface Sci.* **2016**, *21*, 4−13.

https://doi.org/10.1021/acs.jctc.6c00384
J. Chem. Theory Comput. XXXX, XXX, XXX−XXX

(64) Aubret, A.; Ramananarivo, S.; Palacci, J. Eppur si muove, and yet it moves: Patchy (phoretic) swimmers. *Curr. Opin. Colloid Interface Sci.* **2017**, *30*, 81−89.
(65) Gao, Y.; Mou, F.; Feng, Y.; Che, S.; Li, W.; Xu, L.; Guan, J. Dynamic colloidal molecules maneuvered by light-controlled janus micromotors. *ACS Appl. Mater. Interfaces* **2017**, *9*, 22704−22712.
(66) Singh, D. P.; Choudhury, U.; Fischer, P.; Mark, A. G. Non-equilibrium assembly of light-activated colloidal mixtures. *Adv. Mater.* **2017**, *29* (32), 1701328.
(67) Lin, Z.; Si, T.; Wu, Z.; Gao, C.; Lin, X.; He, Q. Lightactivated active colloid ribbons. *Angew. Chem.* **2017**, *129*, 13702−13705.
(68) Theurkauff, I.; Cottin-Bizonne, C.; Palacci, J.; Ybert, C.; Bocquet, L. Dynamic clustering in active colloidal suspensions with chemical signaling. *Phys. Rev. Lett.* **2012**, *108*, 268303.
(69) Pohl, O.; Stark, H. Dynamic clustering and chemotactic collapse of self-phoretic active particles. *Phys. Rev. Lett.* **2014**, *112*, 238303.
(70) Jiang, H.-R.; Yoshinaga, N.; Sano, M. Active motion of a janus particle by self-thermophoresis in a defocused laser beam. *Phys. Rev. Lett.* **2010**, *105*, 268302.
(71) Wang, W.; Duan, W.; Sen, A.; Mallouk, T. E. Catalytically powered dynamic assembly of rod-shaped nanomotors and passive tracer particles. *Proc. Natl. Acad. Sci. U. S. A.* **2013**, *110*, 17744−17749.
(72) Ahmed, S.; Gentekos, D. T.; Fink, C. A.; Mallouk, T. E. Self-assembly of nanorod motors into geometrically regular multimers and their propulsion by ultrasound. *ACS Nano* **2014**, *8*, 11053−11060.
(73) Heinen, L.; Walther, A. Programmable dynamic steady states in atp-driven nonequilibrium dna systems. *Sci. Adv.* **2019**, *5* (7), No. eaaw0590.

https://doi.org/10.1021/acs.jctc.6c00384
J. Chem. Theory Comput. XXXX, XXX, XXX−XXX